

Article

# Numerical Analysis for Hydrogen Flame Acceleration during a Severe Accident in the APR1400 Containment Using a Multi-Dimensional Hydrogen Analysis System

Hyung Seok Kang <sup>1,\*</sup>, Jongtae Kim <sup>2</sup>, Seong Wan Hong <sup>3</sup> and Sang Baik Kim <sup>4</sup>

<sup>1</sup> Korea Atomic Energy Research Institute; hskang3@kaeri.re.kr

<sup>2</sup> Korea Atomic Energy Research Institute; ex-kjt@kaeri.re.kr

<sup>3</sup> Korea Atomic Energy Research Institute; swhong@kaeri.re.kr

<sup>4</sup> Korea Atomic Energy Research Institute; sbkim2@kaeri.re.kr

\* Correspondence: hskang3@kaeri.re.kr; Tel.: +82-42-868-8948 (H.S. Kang)

**Abstract:** Korea Atomic Energy Research Institute (KAERI) established a multi-dimensional hydrogen analysis system to evaluate a hydrogen release, distribution, and combustion in the containment of a nuclear power plant using MAAPI, GASFLOW, and COM3D. KAERI developed the COM3D analysis methodology on the basis of the COM3D validation results against the experiments of ENACCEF and THAI. The proposed analysis methodology accurately predicts the peak overpressure with an error range of approximately  $\pm 10\%$  using the Kawanabe turbulent flame speed model. KAERI performed a hydrogen flame acceleration analysis using the multi-dimensional hydrogen analysis system for a severe accident initiated by a station blackout (SBO) under the assumption of 100% metal-water reaction in the reactor pressure vessel for evaluating an overpressure buildup in the Advanced Power Reactor 1400 MWe (APR1400). The COM3D calculation results using the established analysis methodology showed that the calculated peak pressure in the containment was much lower than the fracture pressure of the APR1400 containment. This calculation result may have resulted from a large air volume of the containment, a reduced hydrogen concentration owing to passive auto-catalytic recombiners installed in the containment, and a lot of stem presence during the hydrogen flame acceleration in the containment. Therefore, we can know that the current design of the APR1400 containment maintains its integrity when the flame acceleration occurs during the severe accident initiated by the SBO accident.

**Keywords:** APR1400; COM3D; Containment Integrity; Hydrogen Flame Acceleration; Multi-Dimensional Hydrogen Analysis System; Overpressure; PAR; Severe Accident

## 1. Introduction

Research into the possibility of a hydrogen explosion, and of a safety device to reduce the hydrogen concentration in the containment of a Nuclear Power Plant (NPP) in Republic of Korea, has been intensively conducted since the hydrogen explosion accident of the NPP in Fukushima in 2011 [1,2]. Thus, Passive Auto-catalytic Recombiners (PARs) were additionally installed in all NPP containments to reduce hydrogen concentration during a severe accident in Republic of Korea [1]. A total of 30 PARs were installed in the Advanced Power Reactor 1400 MWe (APR1400) which had an air free volume of 88,575 m<sup>3</sup> and an opening connection between important compartments in the containment [3,4]. However, the calculation result of a hydrogen distribution assuming 100% metal-water reaction and uncertainty of a hydrogen generation model during the severe accident initiated by a station blackout accident (SBO) in the APR1400 showed the hydrogen concentration is higher than approximately 10% at a local position for an instant time in the containment [3]. Thus, to assure containment integrity, it is necessary to evaluate an overpressure buildup resulting from a

propagation of hydrogen flame along the obstacle and wall in the containment during the severe accidents in the APR1400 accident by the multi-dimensional hydrogen analysis system.

Korea Atomic Energy Research Institute (KAERI) choose the COM3D [5] as the computational code for the overpressure buildup owing to the hydrogen flame acceleration by evaluating for its numerical methods, physical models, a solver algorithm, validation and application results, and its ability to connect an analysis code of a hydrogen distribution in the containment. KAERI has finally established a multi-dimensional hydrogen analysis system for evaluating a hydrogen release, distribution and combustion in the containment of a NPP using MAAP, GASFLOW, and COM3D [6]. The GASFLOW calculates the hydrogen distribution in the containment with a hydrogen source evaluated by the MAAP during the severe accident [7,8]. The COM3D can analyze the overpressure buildup resulting the containment using the hydrogen distribution result calculated by the GASFLOW. It is necessary to evaluate an uncertainty of the COM3D code using a test data before applying it to the hydrogen combustion during the severe accident in the APR1400 containment. In addition, a proper test data for the COM3D validation should be chosen considering the hydrogen and steam concentrations predicted by the GASFLOW and the geometric characteristics of the APR1400 containment to increase the credibility of the COM3D code

## 2. Analysis Methodology for Hydrogen Flame Acceleration

### 2.1. Numerical Models in the COM3D Version 4.10 [5]

The COM3D version 4.10 is a fully explicit finite-differences code on the basis of the well-established numerical methods for solving the compressible Navier-Stokes equation in three-dimensional Cartesian space. The COM3D utilizes a set of transport equations for every gas species and for the total energy, mass, and momentum (Eqs. (1) to (7)). To model a turbulence flow during the hydrogen combustion, the standard k-ε model (Eqs. (8) to (12)) implemented in the COM3D code is used. The COM3D has a recently developed combustion model KYLCOM+ which uses the forest fire algorithm with the burning velocity model for calculating the hydrogen flame propagation. The burning velocity model uses the transport equation of a progressive variable  $f$  such as Eq. (13). The variable  $f = 0$  means a fresh mixture gas, whereas  $f = 1$  means a completely developed reaction. A source term ( $\Phi$ ) to account for the flame propagation owing to a turbulent flow is shown in the transport equation (Eqs. (13) and (14)). A burning criterion,  $F_{i,j,k}$  (Eq. (15)), is used to judge the flame propagation from a burned cell to neighbor cells in the computational domain. If the calculated  $F_{i,j,k}$  in the cell is larger than  $(1/2)^2$ , the flame starts to move from the burned cell to its neighbor cells. The flame propagation speed is predicted by  $C_g$  (Eq. (16)) which is proportional to the gas expansion ratio ( $\sigma$ ) and the turbulent flame speed model ( $S_t$ ). In Eq. (16),  $\alpha$  and  $\beta$  are correlation constants obtained from numerical experiments with the values equal to 0.243 and 0.375, respectively. We choose three turbulent flame models proposed by Bradly (Eq. (17)), Kawanabe (Eq. (18)), and Schmidt (Eq. (19)) in this validation on the basis of the previous COM3D calculation results [9-11]. In three models (Eqs. (17) to (19)),  $S_L$  represents the laminar flame speed dependent on the temperature, pressure, and steam concentration. Eqs. (20) and (21) shows the flammability limit for the diluted steam and its effect to the laminar flame speed. The chemical reaction of the hydrogen-air mixture is calculated by the one-step reaction (Eq. (22)) or the multi-step reaction in the COM3D code, and the calculated combustion energy through the chemical reaction is used as the heat source of the energy equation.

$$\frac{\partial \rho}{\partial t} + \frac{\partial}{\partial x_i} (\rho U_i) = 0 \quad (1)$$

$$\frac{\partial (\rho U_i)}{\partial t} + \frac{\partial}{\partial x_j} (\rho U_i U_j) = -\frac{\partial P}{\partial x_i} + \rho g_i + \frac{\partial M_{ij}}{\partial x_j} \quad (2)$$

$$\frac{\partial(\rho e)}{\partial t} + \frac{\partial}{\partial x_j}((\rho e + p)U_j) = \rho g_j U_j + U_i \frac{\partial M_{ij}}{\partial x_j} + \frac{\partial}{\partial x_j} \left( \frac{\mu_{nr}}{C_h} \frac{\partial}{\partial x_j} \left( e - \frac{1}{2} U_i U_i + \frac{P}{\rho} \right) \right) + B + \rho \varepsilon \quad (3)$$

$$M_{ij} = -\frac{2}{3} \delta_{ij} \left( \rho k + \mu_{nr} \frac{\partial U_r}{\partial x_r} \right) + \mu_{nr} \left( \frac{\partial U_i}{\partial x_j} + \frac{\partial U_j}{\partial x_i} \right) \quad (4)$$

$$\frac{\partial(\rho Y_\alpha)}{\partial t} + \frac{\partial}{\partial x_j}(\rho Y_\alpha U_j) = \bar{\omega}_\alpha + \frac{\partial}{\partial x_j} \left( \frac{\mu_{nr}}{C_{f\alpha}} \frac{\partial Y_\alpha}{\partial x_j} \right) \quad (5)$$

$$e = \sum_{\alpha=1}^N \frac{Y_\alpha}{\mu_\alpha} (h_\alpha + \Delta h_\alpha^0 - RT) + \frac{1}{2} U_i U_i \quad (6)$$

$$Y_\alpha = \frac{\rho_\alpha}{\rho} \quad (7)$$

$$\frac{\partial(\rho k)}{\partial t} + \frac{\partial}{\partial x_j}(\rho k U_j) = S - \rho \varepsilon + \frac{\partial}{\partial x_j} \left( \frac{\mu_{nr}}{C_k} \frac{\partial k}{\partial x_j} \right) \quad (8)$$

$$\frac{\partial(\rho \varepsilon)}{\partial t} + \frac{\partial}{\partial x_j}(\rho \varepsilon U_j) = \left( \frac{\varepsilon}{k} C_1 S - C_2 \rho \varepsilon \right) + \frac{\partial}{\partial x_j} \left( \frac{\mu_{nr}}{C_\varepsilon} \frac{\partial \varepsilon}{\partial x_j} \right) \quad (9)$$

$$S = \frac{\partial U_i}{\partial x_j} M_{ij} - B \quad (10)$$

$$\mu_{nr} = \mu + C_\mu \rho \frac{k^2}{\varepsilon} \quad (11)$$

$$B = \frac{\mu_{nr}}{C_\rho} \frac{1}{\rho^2} \frac{\partial \rho}{\partial x_r} \frac{\partial P}{\partial x_r} \quad (12)$$

$$\frac{\partial \rho f}{\partial t} + \frac{\partial \rho u_i f}{\partial x_i} = \frac{\partial}{\partial x_i} \left( \rho D_i \frac{\partial f}{\partial x_i} \right) + \Phi \quad (13)$$

$$\Phi = \begin{cases} \frac{\rho C_g}{\Delta} (1 - f_{i,j,k}) & F_{i,j,k} > \left(\frac{1}{2}\right)^2 \\ 0 & F_{i,j,k} < \left(\frac{1}{2}\right)^2 \end{cases} \quad (14)$$

$$F_{i,j,k} = f_{i+1,j,k}^2 + f_{i-1,j,k}^2 + f_{i,j+1,k}^2 + f_{i,j-1,k}^2 + f_{i,j,k+1}^2 + f_{i,j,k-1}^2 - 3f_{i,j,k}^2 \quad (15)$$

$$C_g = (\alpha \cdot \sigma + \beta) S_t \quad (16)$$

$$S_t^{Bradly} = S_L \left( \sqrt{\frac{u'}{S_L}} \left( \frac{LS_L}{\chi} \right)^{\frac{1}{6}} \right) \quad (17)$$

$$S_t^{Kawanabe} = S_L \left( 1 + 1.25 \left( \frac{u'}{S_L} \right) \right)^{0.7} \quad (18)$$

$$S_t^{Schmidt} = S_L + \frac{u'}{\sqrt{1 + \frac{1}{Da^2}}} \quad (19)$$

$$S_{L,steam}(T) = S_{L,air}(T) \sqrt{\frac{\lambda_{steam}(T)}{\lambda_{air}(T)}} \left( 1 - \frac{X_{H_2,steam}}{X_{L,steam}} \right) \quad (20)$$

$$X_{L,steam} = 0.5 - 0.2443 \ln(X_{H_2,air}) - 0.185 (\ln(X_{H_2,air}))^2 \quad (21)$$



## 2.2. COM3D Validation

The test data of the hydrogen combustion performed at the ENACCEF and THAI facilities were chosen for evaluating the uncertainty of the COM3D code and determining the proper turbulent flame speed model to simulate the hydrogen flame acceleration during the severe accident in the APR1400 containment.

### 2.2.1. ENACCEF Test

IRSN in France performed the hydrogen flame acceleration test using the ENACCEF facility with the hydrogen concentration of 13% and the obstacle blockage ratio of 0.63 (Table 1) [12]. The ENACCEF is a vertical facility of 5 m high as shown in Figure 1. It is divided into two parts of the acceleration tube and the dome region. Nine annular obstacles are continually installed in the acceleration tube. The first obstacle is located at 0.876 m from the bottom of the acceleration tube. The blockage ratio of the obstacle is defined as Eq. (23). In the equation, D and d are the inner diameters of the acceleration tube and obstacle, respectively. The hydrogen-air mixture was ignited at the bottom region by an electric spark device after setting the initial hydrogen concentrations. Then, the hydrogen flame propagated upward along the acceleration tube in the test facility. They measured the flame front time of arrival (TOA) at 16 locations using photomultiplier tubes and the pressure at 9 locations to observe the flame acceleration phenomenon using high-speed pressure transducers.

$$BR = 1 - (d/D)^2 \quad (23)$$

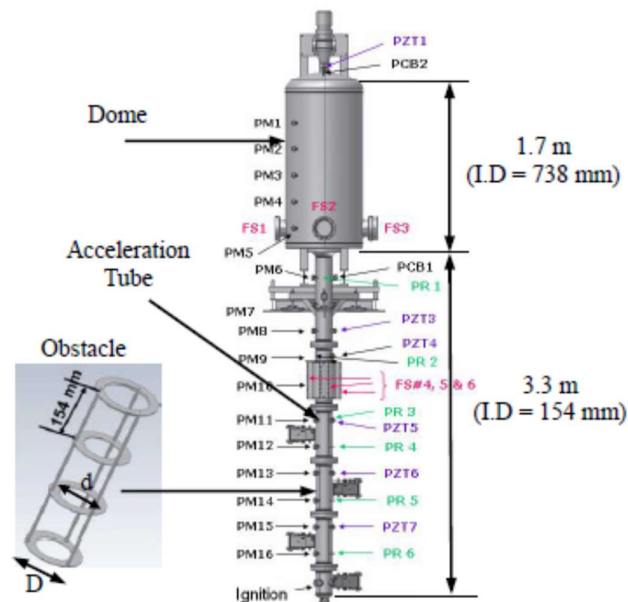
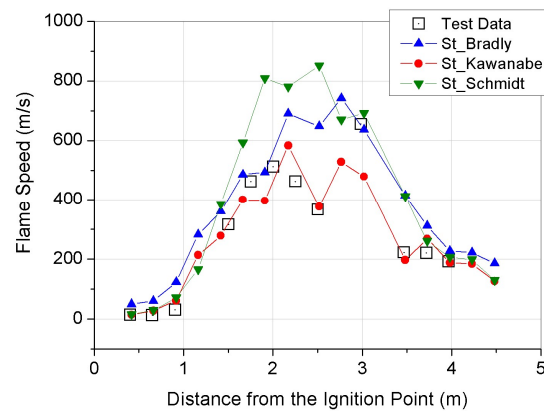


Figure 1. ENACCEF Facility [12]

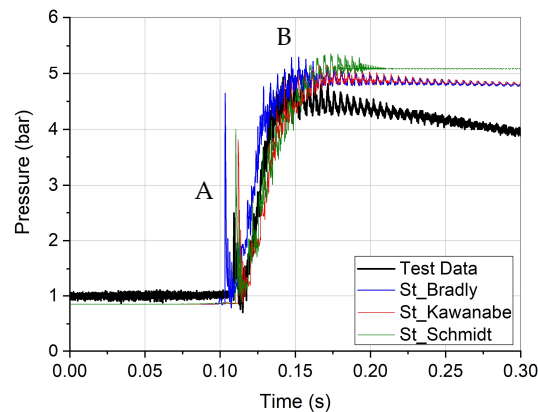
Table 1. Initial condition of the ENACCEF RUN153 Test [12].

Case	H <sub>2</sub> Con. (%)	Steam Con. (%)	Air Con. (%)	Temp (°C)	Pressure (bar)
RUN153	13	0	87	25	1.0

The COM3D analysis was performed for the ENACCEF test to estimate the uncertainty of the COM3D prediction according to the turbulent flame speed models of Bradley, Kawanabe, and Schmidt. A turbulent flow in the combustion flow field was modeled using the standard  $k-\epsilon$  turbulent model and low Reynolds wall function model. One step  $H_2$ -Air chemical reaction model (Eq. (22)) was used with the KYLCOM+ combustion model. An ignition process was modeled by the use of a hot spot spherical region with a radius of 30.8 mm where the hydrogen-air chemical reaction takes place with a laminar flame speed. A 3-dimensional grid model with a quarter symmetric condition was generated for simulating the ENACCEF test facility. A total of 439,217 hexahedral cells with a cell length of 7.7 mm were generated in the grid model. A slip wall condition was applied to reduce the number mesh distribution near the wall. A wall condition with a constant temperature of 298 K was applied on the outer surface of the grid model. The time step size for the COM3D calculations was automatically controlled to assure a Courant-Friedrichs-Lewy (CFL) number below 0.9.



(a) Comparison of flame speed between the test data and the COM3D results



(b) Comparison of pressure between the test data and the COM3D results

**Figure 2.** COM3D results for ENACCEF Test

The test results showed that the flame acceleration through the obstacles induced the pressure buildups measured at PCB2 in Figure 2. The first pressure peak (A) occurred by a compression effect when the hydrogen flame front arrived at the dome entrance. The second pressure peak (B) was developed at around the end of the hydrogen-air chemical reaction in the dome region. After the end of the hydrogen combustion, the pressure started to decrease by a heat loss from the ENACCEF wall into the air environment. The flame arrival time needed for calculating the flame speed in the COM3D calculation was defined as the instant when the gas temperature increases to approximately 700 K at the locations of PM1 to PM16. The comparison between the COM3D result and test data shows that the KYLCOM+ model with the Kawanabe correlation accurately predicts the flame speed and peak pressure with an error range of about  $\pm 10\%$  (Figure 2). However, the COM3D results overpredict the pressure behavior from 0.15 s to 0.30 s in Figure 2(b). This overestimation may have resulted from the

higher flame temperature owing to the less heat transfer from the hydrogen flame to the test facility wall because the COM3D does not have a steam condensation model along the wall and a radiative heat transfer model. We did not perform the grid sensitivity analysis for this problem because AREVA already conducted the grid dependency study for the ENACCEF test results with the COM3D in the ISP-49 benchmark problem [13]. They finally addressed that the COM3D has no significant grid dependency in the analysis of the ENACCEF test results when the cell size of approximately 10 mm was used for the grid model.

### 2.2.2. THAI Test

Becker Technologies in Germany performed the hydrogen deflagration test at the condition of the hydrogen concentration of approximately 10% with varying the steam concentration from 0% to 25% in the THAI facility [14]. The THAI facility is a cylindrical stainless steel vessel of 9.2 m height and 3.2 m diameter with a total volume of 60 m<sup>3</sup> as shown in Figure 3. The vessel outer wall is completely enveloped by a 120 mm rockwool thermal insulation. An obstacle geometry to accelerate the hydrogen flame was not installed, but a structure to support thermocouples was existed in the vessel. An air-driven axial fan installed in the lower plenum of the vessel was used to set homogenization of the vessel gas atmosphere prior to the start of the hydrogen combustion. To monitor the gas temperature change during hydrogen deflagration, 43 thermocouples (TCs) with outer diameter 0.25 mm were installed at 13 different elevations in the vessel. The gas temperatures were measured at the rate of 1000 Hz. The hydrogen-air mixture was ignited at the bottom region by an electric spark device after setting the initial hydrogen concentrations as shown in Table 2. Then, the hydrogen flame propagated upward along the acceleration tube in the test facility.

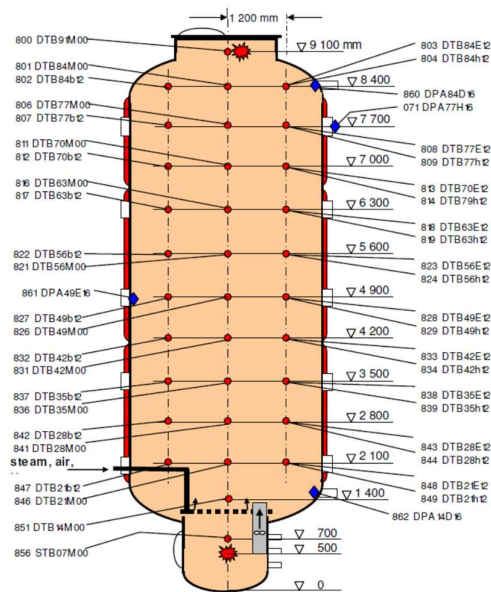
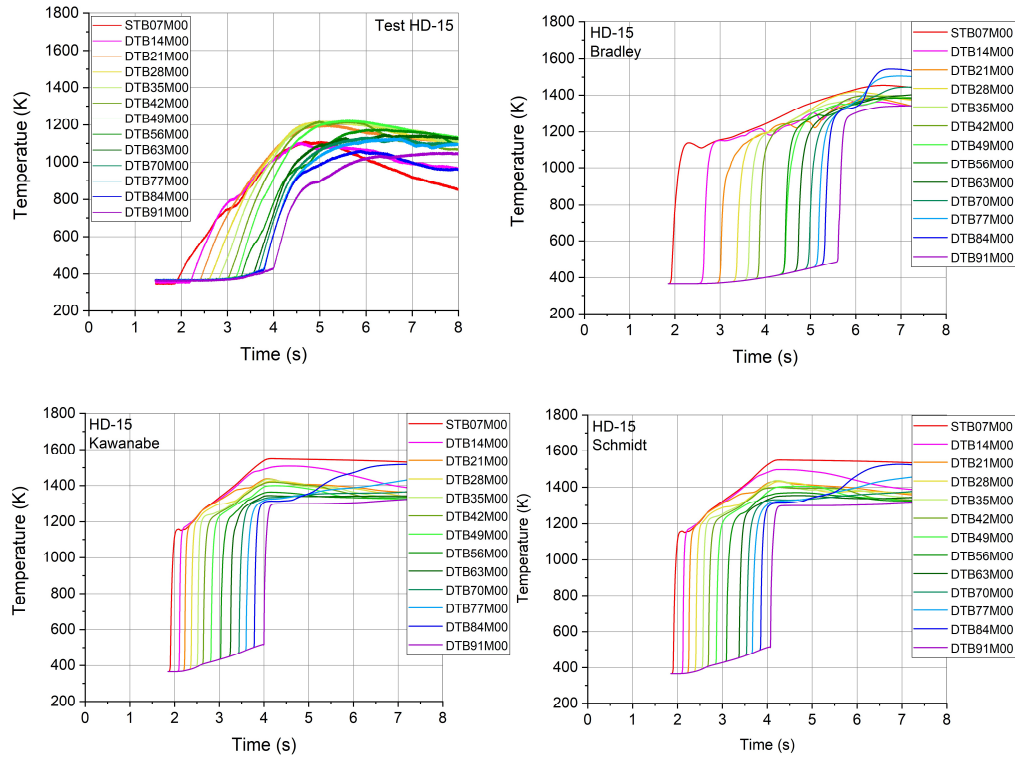


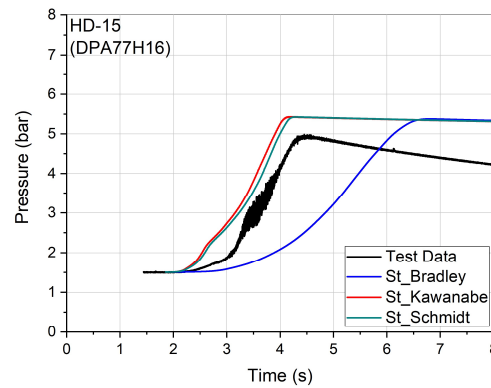
Figure 3. THAI facility [14]

Table 2. Initial conditions of THAI HD-15 and HD-22 Test [14].

Case	H <sub>2</sub> Con. (%)	Steam Con. (%)	Air Con. (%)	Temp (°C)	Pressure (bar)
HD-15	9.93	0	90.07	92.5	1.50
HD-22	9.90	25	65.10	91.9	1.48

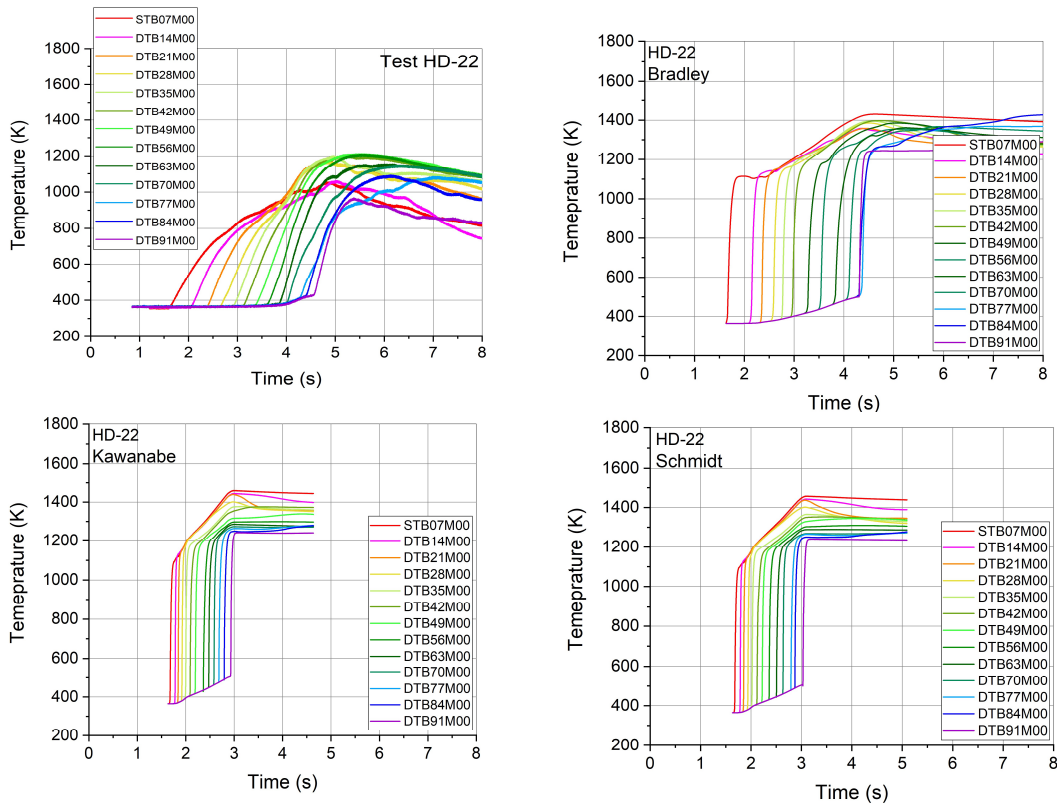


(a) Measured and calculated temperatures along the centerline of the vessel

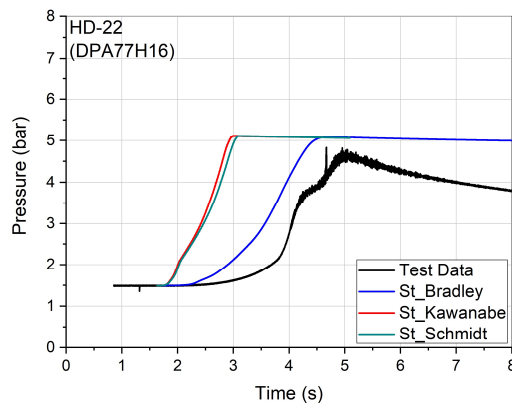


(b) Comparison of pressure at the elevation 7.7 m between the test data and the COM3D results

**Figure 4. COM3D results for the THAI test HD-15**



(a) Measured and calculated temperatures along the centerline of the vessel



(b) Comparison of pressure at the elevation 7.7 m between the test data and the COM3D results

Figure 5. COM3D results for the THAI test HD-22

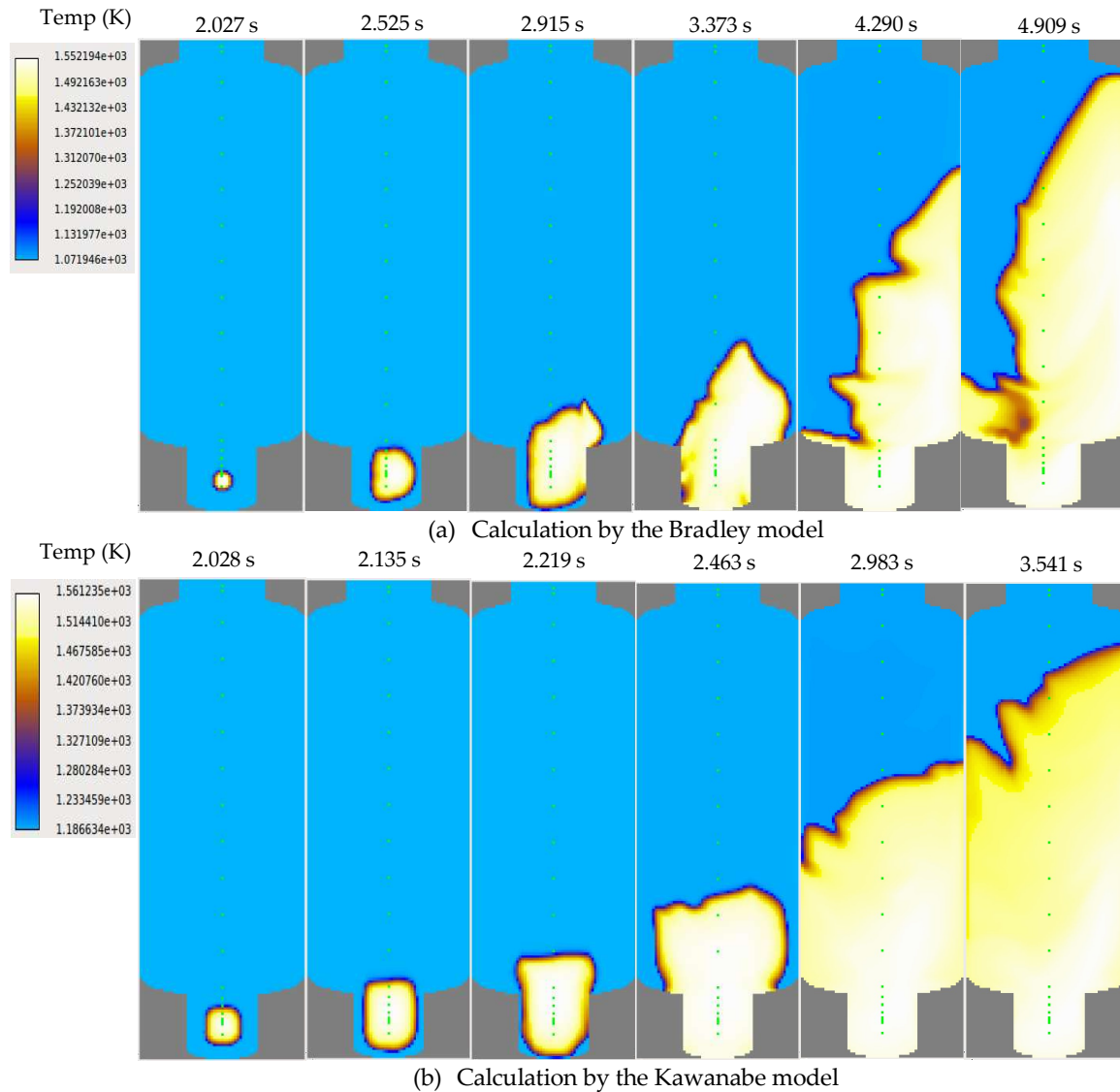


**Figure 6. Temperature Contours on the Center Plane for the Test HD-15 by COM3D**

The flame speed data was not provided in the test HD-15 and HD-22. Thus, we decided to use a time needed for the flame propagation on the basis of the measured temperature data as a parameter to see the characteristics of the hydrogen flame. The test results showed that the time needed for the flame propagation along the centerline from 0.7 m to 9.1 m in the vessel was increased from approximately 1.5 s to 2.0 s as the steam concentration increased from 0% to 25% as shown in Figures 4(a) and 5(a). In this estimation, we assumed that the flame front arrived when the gas temperature increased to approximately 700 K at the TC locations along the centerline in the vessel. However, the maximum temperatures at the elevation 0.7 m to 9.1 m along the centerline were decreased from approximately 30 K to 70 K as the steam concentration increased. This may be explained by the fact that more hydrogen combustion energy was used to increase the temperature of the mixture gas of the hydrogen-air and steam in the test HD-22 because the specific heat of the mixture gas of the hydrogen-air and steam was increased to approximately 20% from those of the mixture gas of the hydrogen-air in the test HD-15 [15]. As the results of this maximum temperature change, the peak pressure at elevation 7.7 m in the vessel was decreased from approximately 5.0 bar to 4.6 bar as the steam concentration increased such as Figures 4(b) and 5(b). After the end of the hydrogen combustion in the

test, the temperatures and pressure started to decrease by the heat loss from the THAI vessel wall into the air environment like as the ENACCEF test.

The COM3D analyses for the HD-15 and HD-22 tests were performed to measure an effect of steam presence on the hydrogen deflagration analysis using the same models and method as used for the ENACCEF analysis. A full 3-dimensional grid model was generated for simulating the THAI vessel. A total of 481,928 hexahedral cells with a cell length of 50 mm were generated in the grid model on the basis of the previous COM3D analysis for the THAI experiments [9,11]. A wall condition with a constant temperature of 298 K was applied on the outer surface of the grid model. The ignition process was modeled by the use of a hot spot spherical region with a radius of 0.1 m where the hydrogen-air chemical reaction takes place with a laminar flame speed. The comparison of temperatures and pressure between the COM3D results and test data are shown in Figures 4 and 5. The COM3D results with the KYLCOM+ model using the turbulent flame speed models of Bradley, Kawanabe, and Schmidt show that the pressure decrease according to the steam concentration increase from 0% to 25% are all accurately predicted from approximately 5.5 bar to 5.0 bar with an error range of approximately 10% compared to the test data such as Figures 4(b) and 5(b). However, the time needed for the flame propagation along the centerline from 0.7 m to 9.1 m in the test HD-22 is decreased to approximately 75% of the calculated results for the test HD-15. These results are different from the measured data in the tests HD-15 and HD-22. This means that the flame propagation becomes faster as the steam concentration increases from 0% to 25%. To find the exact reason for this problem, we will investigate the laminar flame speed model at the steam presence implemented in the COM3D version 4.10 [11]. The time needed for the flame propagation using the Bradley model is longer than those of others models as shown in Figures 4(a) and 5(a). This result may be explained by the fact that the hydrogen flame first propagates along the right side wall and moves upward to the central region in the vessel in the COM3D analysis with the Bradley model such as Figure 6(a). The temperature contours on the center plane of the vessel by the Kawanabe model show that the flame mainly propagates upward along the central plane in the vessel (Figure 6(b)). The flame propagation by the Schmidt model is similar to that of the Kawanabe model (Figure 4(a)). Through the COM3D analyses for the tests of HD-15 and HD-22, we find that the calculated peak pressures by the COM3D accurately predict the measured pressures with an error range of about  $\pm 10\%$  even though the times needed for the flame propagations are oppositely predicted. However, the COM3D results overestimate the pressure after completing the hydrogen combustion like as the analysis result for the ENACCEF test.

### 2.3. Proposed Analysis Methodology for the Hydrogen Flame Acceleration

KAERI established the COM3D analysis methodology (Table 2) on the basis of the COM3D validation results against the test data of ENACCEF and THAI. The proposed analysis methodology accurately predicted the peak overpressure with an error range of approximately  $\pm 10\%$ . However, the COM3D analysis results did not accurately predict the time needed for the flame propagation under the condition of the steam presence in the THAI facility.

**Table 2.** Proposed COM3D Analysis Methodology for the Hydrogen Flame Acceleration.

Parameter	Model
• Explicit solver	2 <sup>nd</sup> order Total Variation Diminishing
• Combustion model	KYLCOM+
• Turbulent flame speed model	Kawanabe
• Wall function	Low Re number
• CFL number	< 0.9
• RED number	< 0.4

### 3. Application to the Severe Accident of the APR1400

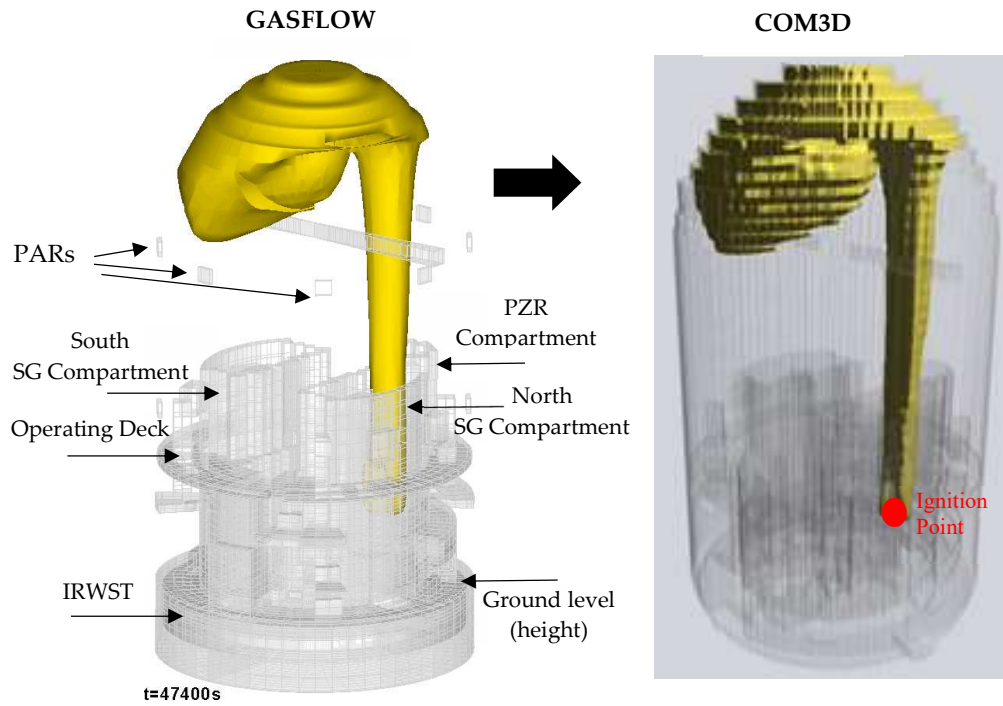
#### 3.1 Design Feature of the APR1400 Containment

There are two plants of APR1400 which are currently operating and four plants are being constructed in Koera. The dimension of the APR1400 containment was changed to include the in-containment refueling water storage tank (IRWST) in the containment, which was located at the outside of the containment of the Optimised Power Reactor 1000 MWe (OPR1000). Thus, the diameter and height of the APR1400 containment with a cylindrical dome geometry were increased to 45.72 m and 69.69 m from 43.89 m and 65.83 m in the OPR1000, respectively. The containment height is defined from the ground level to the top of the cylindrical dome. As a result of this geometrical change, the air free volume in the APR1400 containment was also increased to approximately 88,631 m<sup>3</sup> from 77,021 m<sup>3</sup> of the OPR1000. In addition, the top and bottom of the SG compartments in the APR1400 and OPR1000 were opened to the air free space in the containments. The APR1400 has a safety depressurization system (SDS) which discharges the reactor coolant from the primary system to the IRWST to reduce the primary system pressure during a high pressure accident like as the SBO. A 3-way valve located at the bottom of the pressurizer (PZR) in the SDS changes the flow path of the discharge of the reactor coolant from the IRWST to the north SG compartment when the severe accident occurred in the reactor pressure vessel (RPV) during the SBO accident for preventing the hydrogen release to the IRWST according to the severe accident management guideline (SMAG) [4]. In this study, the release location of the hydrogen in the SG compartment was assumed as the elevation similar to the bottom of the PZR. The released hydrogen gas into the containment may be removed by the thirty passive auto-catalytic recombiners (PARs) installed in the containment though the electrical power is not available during the SBO accident. The design pressure of the inner wall in the APR1400 containment is approximately 513 kPa in absolute pressure.

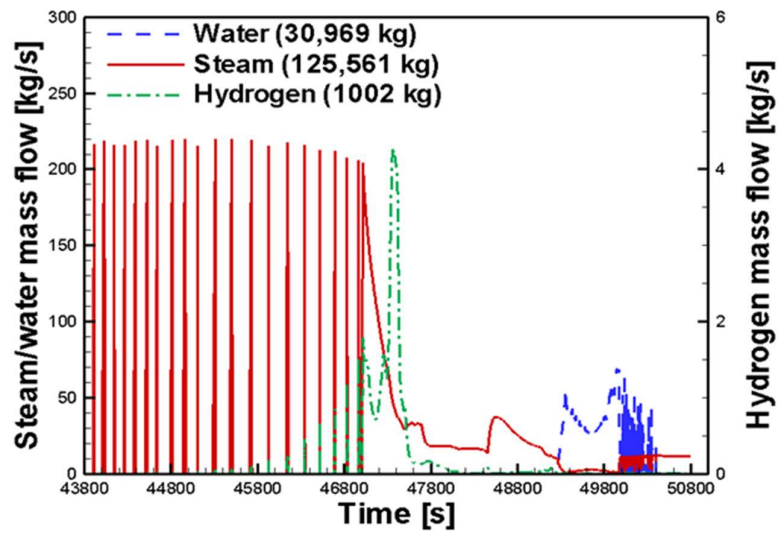
#### 3.2. Calculation of the Hydrogen Distribution by GASFLOW and MAAP

To evaluate an overpressure buildup owing to the hydrogen flame acceleration during the severe accident initiated by the SBO in the APR1400 containment by the COM3D code, the calculation of the hydrogen distribution in the containment by the GASFLOW was first performed using the hydrogen and steam generation rate (Figure 7(b)) which was obtained under the assumption of a 100% metal-water reaction in the RPV considering the uncertainty of the hydrogen generation model in the MAAP code. The total generated hydrogen mass in the RPV by MAAP was 1002 kg which was calculated by imposing the uncertainty 50% to the zirconium oxidation rate. This mass was approximately 83% of the maximum hydrogen mass which can be generated through the zirconium oxidation in the RPV. Figure 7(b) shows that a lot of steam is released to the containment from the RPV before the hydrogen discharges. The GASFLOW results at 47,400 s and its grid model representing the APR1400 containment, as shown in Figure 7(a), were transferred from the GASFLOW to the COM3D because the calculated sigma cloud by the GASFLOW revealed the possibility of hydrogen flame acceleration over the long distance [3]. The amount of hydrogen, oxygen, and steam transferred from the GASFLOW results at 47,400 s are 694.7 kg, 24,375 kg, and 48,760 kg, respectively. Figure 8 shows the initial conditions of the gas concentrations, temperature, pressure, and turbulence for the COM3D calculation after transferring from the GASFLOW results. According to the distributions of the mixture gas of the hydrogen and air, the flame acceleration may sufficiently occur along the mixture gas vertical column with approximately 0.5 m diameter and 57 m length [16]. When the grid model was transferred from the GASFLOW to the COM3D, its cell length was decreased to approximately 50 cm from 100 cm to accurately resolve the pressure wave propagation generated from the combusted region, model the important structures to the hydrogen flame acceleration in the containment, and complete the calculation of the hydrogen flame acceleration in the proper time [10,11]. Therefore, a total of 1,453,025 hexahedral cells in the grid model were generated for the calculation of the hydrogen flame acceleration. The wall condition with a constant temperature of 298 K was applied to the outer surface of the grid model. The air free volume in the grid model for the COM3D analysis is approximately

92,943 m<sup>3</sup> which is approximately 4.8% larger than the design value of the air free space in the APR1400 [4].

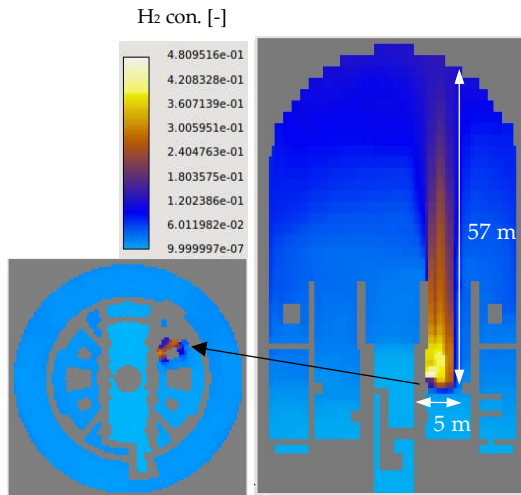


(a) Iso-surface of H<sub>2</sub> 10% in the grid model of CASFLOW and COM3D

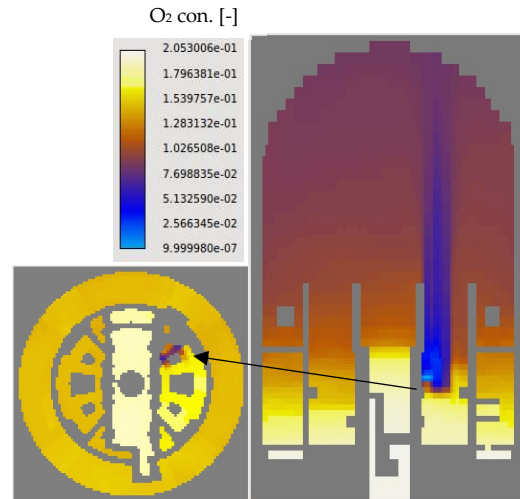


(b) Predicted hydrogen and steam generation rate by MAAP

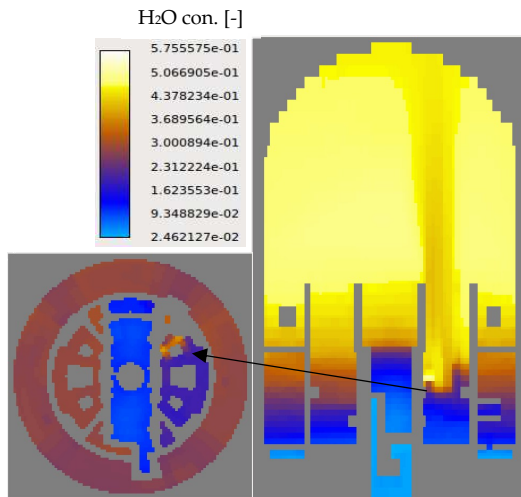
Figure 7. MAAP and GASFLOW results for the SBO accident



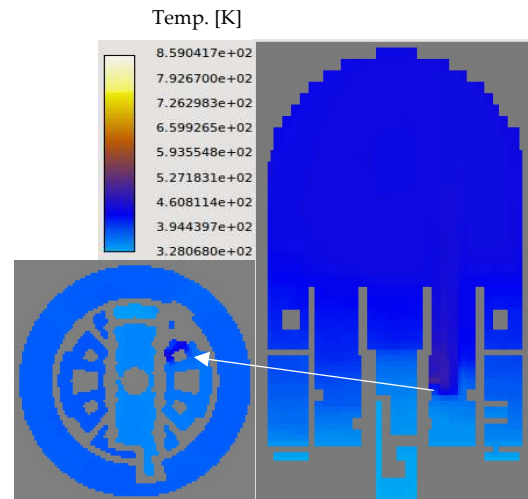
(a) Hydrogen Concentration



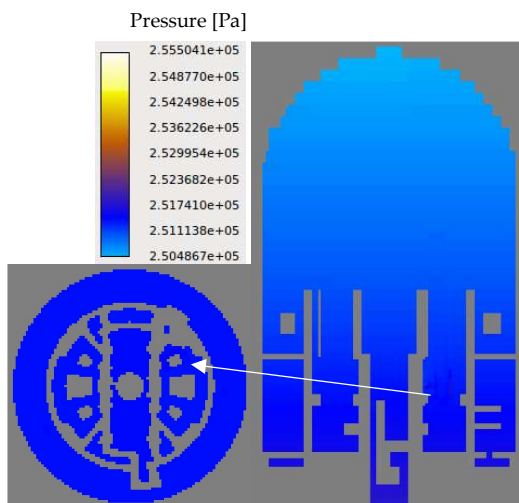
(b) Oxygen Concentration



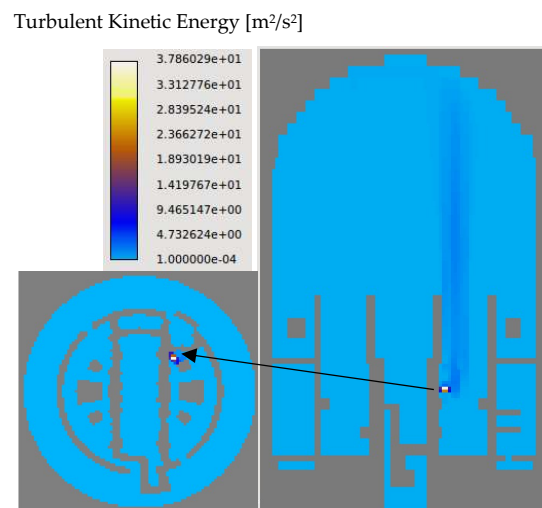
(c) Steam Concentration



(d) Temperature



(e) Pressure



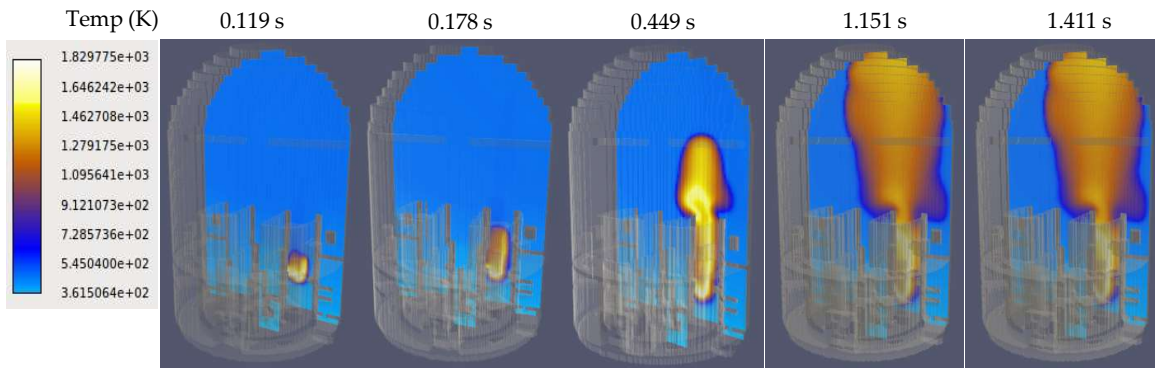
(f) Turbulent Kinetic Energy

### Figure 8. Initial Conditions of the COM3D Calculation for the Severe Accident

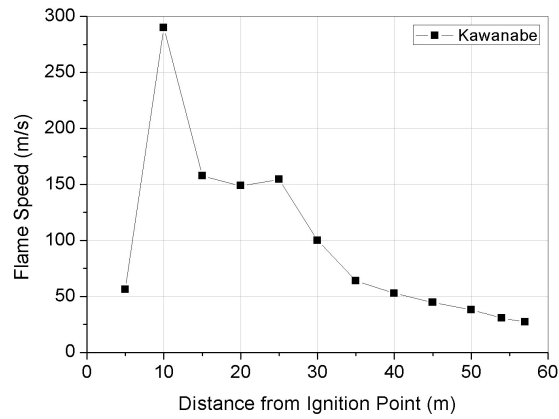
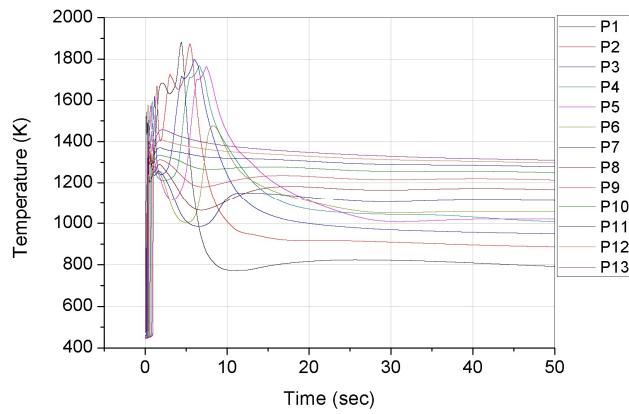
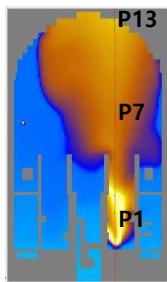
#### 3.3. Calculation of the Hydrogen Flame Acceleration by the COM3D Code

The COM3D calculation for the hydrogen flame acceleration during the severe accident in the APR1400 containment was performed using the transferred GAFLOW results and refined grid model on the basis of the proposed the COM3D analysis methodology (Table 2). In particular, to induce a strong flame acceleration over a long distance, the ignition point was assumed at around the hydrogen release location in the north SG compartment (Figure 7(a)) [17]. The ignition process was modeled by the use of a hot spot spherical region with a radius of 0.5 m where the hydrogen-air chemical reaction takes place with a laminar flame speed. The COM3D results using the Kawanabe models shows that the hydrogen flame is propagated to approximately 57 m along the vertical direction in 1.10 s after the start of the ignition and turns its direction to the left side where the hydrogen is located as shown in Figure 9(a). The calculated flame speeds between from P1 to P3 are increased to approximately 300 m/s in the SG compartment and decreased to about 30 m/s at the upper region of the containment (Figure 9(b)). This flame speed variation along the vertical direction may have resulted from the initial conditions of the hydrogen, oxygen, and steam concentrations and turbulent kinetic energy (Figure 8) because the turbulent flame speed is calculated by using the combusted energy and turbulent intensity. The flame arrival time needed for calculating the flame speed is defined as the instant when the gas temperature increases to approximately 700 K at the locations of P1 to P13. The calculated flame speed of approximately 300 m/s around the hydrogen release point in the SG compartment looks like a lower speed when considering the hydrogen concentration of approximately 25% to 35% as shown in Figure 8(a). This result may be explained by the fact that the oxygen with approximately 4% to 7% locating around the hydrogen release point limits the total hydrogen mass consumed in the chemical reaction of the hydrogen and air such as Eq. (22). Thus, the calculated combustion energy may be similar to that of the hydrogen concentration of approximately 8% to 14%.

In addition, the steam presence with approximately 35% to 45% hinders the hydrogen-air chemical reaction at around the hydrogen release point. As a result of this oxygen starvation phenomenon, the hydrogen with approximately 15% to 20% still remains after the flame front arrives at the upper location of the top of the SG compartment (Figure 10). According to the hydrogen combustion effected by the oxygen starvation in the SG compartment, the increased pressures owing to the weak flame acceleration during the severe accident initiated by the SBO are approximately 260 kPa from the initial pressure of approximately 250 kPa such as Figure 11(a). This low pressure increase may have resulted from the low flame speed along the vertical hydrogen column. Another reason is believed that the pressure wave generated at the combusted region passes through the open spaces in the upper region of the large containment as shown in Figure 11(b). If the COM3D can simulate the steam condensation along the containment wall, the peak pressure may be decreased from approximately 510 kPa. Through the hydrogen combustion calculation, we find that the calculated peak pressure in the containment by the COM3D does not exceed the fracture pressure 1223 kPa in absolute pressure which is imposing on the inner wall of the APR1400 containment [4]. The fracture pressure is generally assumed as approximately 2.38 times of the design pressure of the containment.



(a) Temperature distribution as time passes



(b) Temperature behaviors and flame speeds from P1 to P13

Figure 9. Predicted Temperature for the Hydrogen Flame Acceleration by COM3D

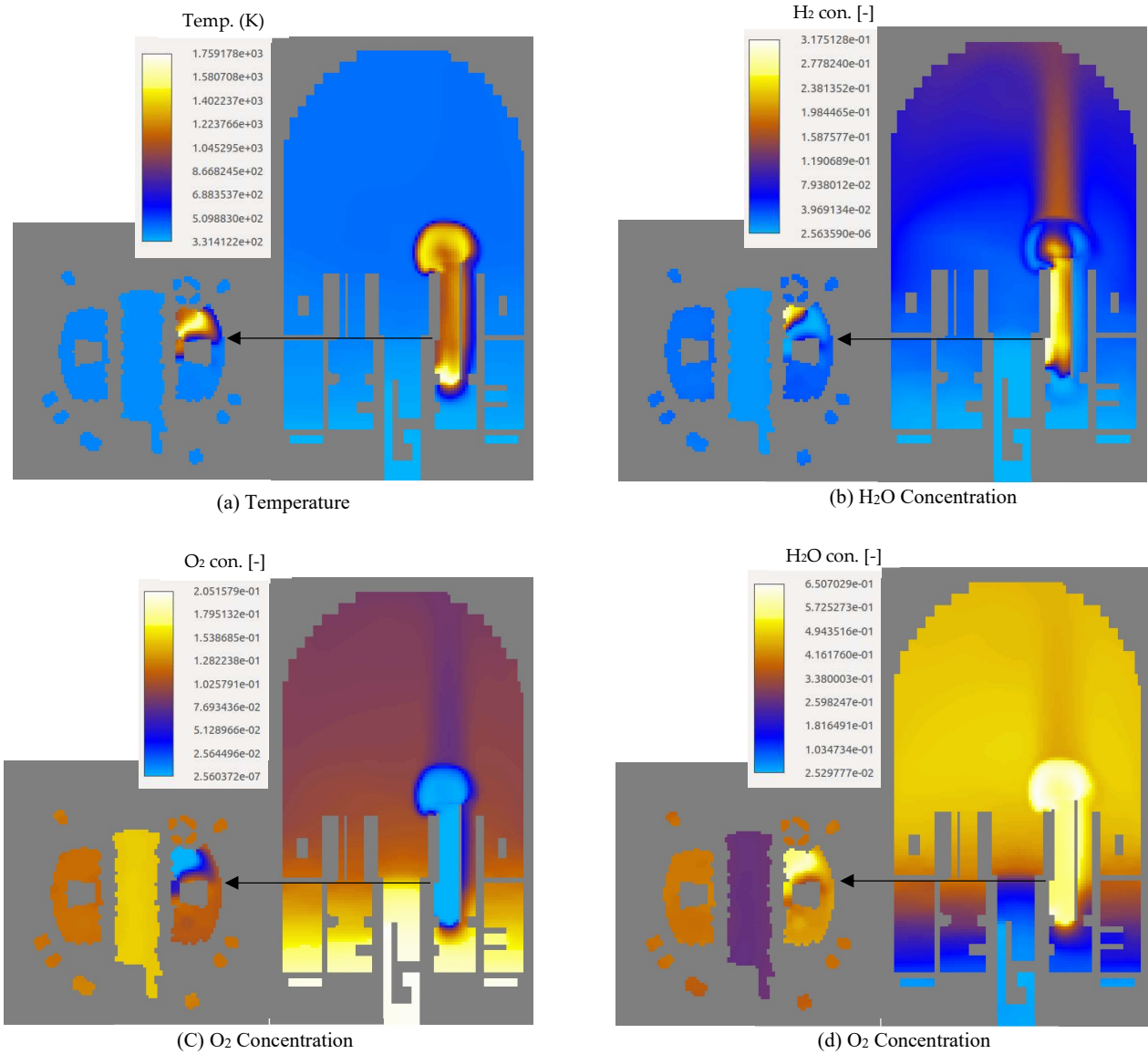


Figure 10. Predicted Gas Concentrations and Temperature at 0.278 s during the Hydrogen Flame Acceleration

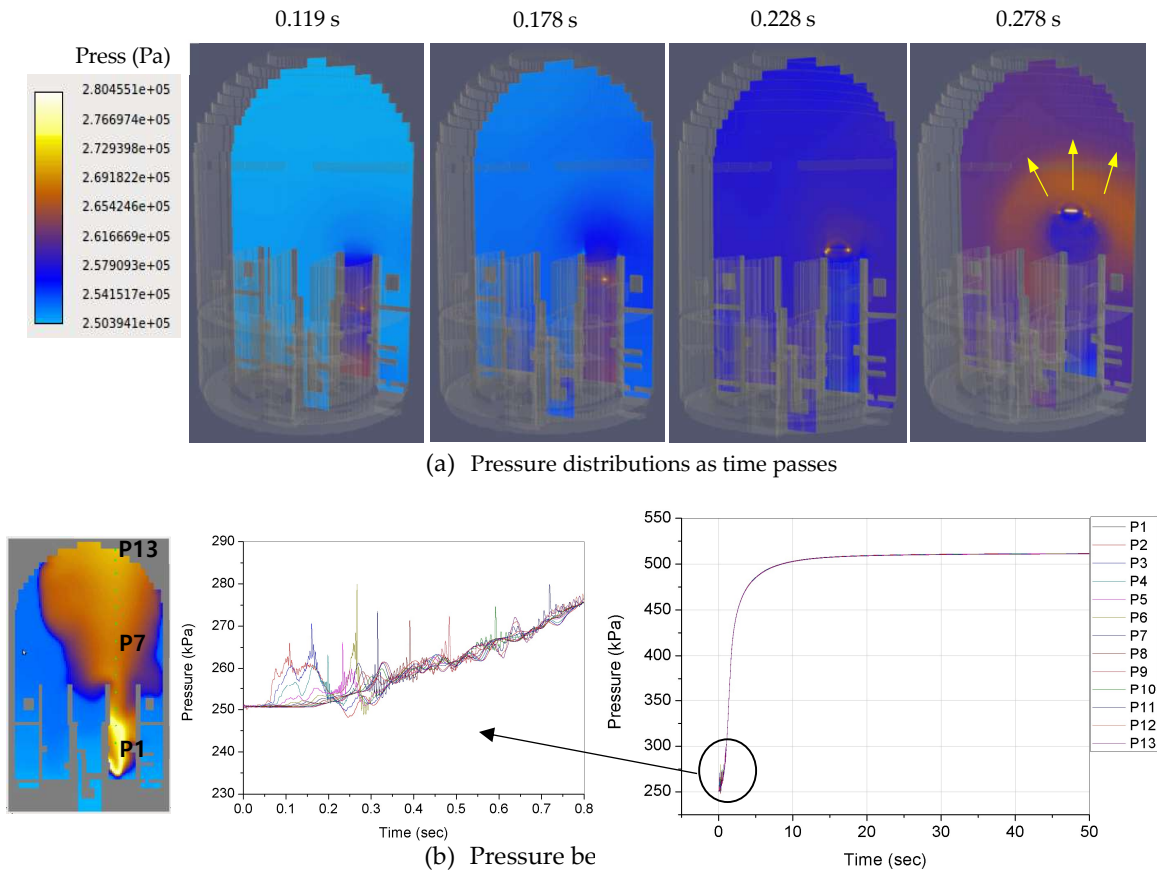


Figure 11. Predicted pressure for the hydrogen flame acceleration by COM3D

#### 4. Conclusion and Further Work

We established a multi-dimensional hydrogen analysis system for evaluating a hydrogen release, distribution and combustion in the containment of a NPP using MAAP, GASFLOW, and COM3D. KAERI performed a COM3D analysis for the ENACCEF and THAI tests to estimate the uncertainty of the COM3D prediction according to the turbulent flame speed models of Bradley, Kawanabe, and Schmidt. Through the COM3D analysis for the ENACCEF and THAI tests, we developed the COM3D analysis methodology predicting the peak pressure with an error range of approximately  $\pm 10\%$ . We analyzed the hydrogen flame acceleration accident in the APR1400 containment during the severe accident initiated by the SBO using the multi-dimensional hydrogen analysis system on the basis of the proposed the COM3D analysis methodology. In particular, to induce a strong flame acceleration over a long distance, the ignition point was assumed at around the hydrogen release location in the SG compartment. From the COM3D calculation results, we found that the pressure buildup was approximately 250 kPa from the initial pressure of the COM3D calculation because the flame speed was not increased above 300 m/s and the pressure wave passed through the open spaces in the upper region of the large containment. The COM3D results showed that the calculated peak pressure in the containment is much lower than the fracture pressure of the APR1400 containment. As a further work, we will have to investigate the laminar flame speed model under the steam presence implemented in the COM3D version 4.10 for more accurate prediction for the THAI test HD-22. In addition, we will perform the COM3D analysis against a large scale test of the hydrogen combustion to increase the applicability of the COM3D analysis to the NPP containment.

**Acknowledgments:** This work was supported by the National Research Foundation of Korea (NRF) grant funded by the Korea government (Ministry of Science, ICT, and Future Planning) (No. 2017M2A8A4015277).

## Nomenclature

$D_a$	Damköhler number
$D_t$	turbulent diffusion coefficient [ $m^2/s$ ]
$e$	internal energy [J]
$f$	progressive variable [-]
$g$	gravity [ $m/s^2$ ]
$h$	enthalpy [J]
$k$	turbulent kinetic energy [ $m^2/s^2$ ]
$L$	integral length scale [m]
$P$	pressure [Pa]
$R$	gas constant [J/kgK]
$S_L$	laminar flame speed [m/s]
$S_t$	turbulent flame speed [m/s]
$T$	temperature [K]
$u'$	turbulence intensity [m/s]
$U_i$	velocity component [m/s]
$Y_\alpha$	mass fraction of species $\alpha$ [-]

### Greek letters

$\alpha, \beta$	correlation constant [-]
$\varepsilon$	turbulent eddy dissipation [ $m^2/s^2$ ]
$\mu$	viscosity [kg/ms]
$\lambda$	thermal conductivity [W/mK]
$\rho$	density [ $kg/m^3$ ]
$\omega$	reaction rate per unit volume [ $kg/m^3s$ ]
$\chi$	thermal conductivity of mixture gas [W/mK]
$\sigma$	gas expansion coefficient [-]

### Subscripts

tur	turbulence
t	turbulence

## References

1. Severe Accident Research Committee. Status of Follow-up Action from Fukushima Accident, Workshop of Korea Nuclear Society, Jeju, Korea, May 16-18, 2012.
2. Nuclear Safety and Security Commission. Status of Follow-up Measures and Action Plan from Fukushima Accident, 23<sup>rd</sup> Committee Meeting, Seoul, Korea, March 14, 2014.
3. Kim, J.; Hong, S.W., Analysis of Hydrogen Flame Acceleration in APR1400 Containment by Coupling hydrogen Distribution and Combustion Analysis Codes. *Progress in Nuclear Energy* **2015**, *78*, pp. 101-109.
4. Korea Hydro & Nuclear Power. Final Safety Analysis Report of Shin-Kori 1&2, 2012.
5. Kotchourko, A.; Lelyakin, J.; Yanez, J.; Halmer, G.; Svishchev, Z.; Xu, Z.; Ren, K. COM3D User/Tutorial Guide, Version 4.10, KIT, Germany, 2015.
6. Kang, H.S.; Kim, J.; Hong, S.W. Evaluation and Selection of a multi-Dimensional Computational Code for a Hydrogen Combustion and Explosion in the Containment of a Nuclear Power Plant, Technical Report, KAERI, Korea, 2013.
7. Henry, R.E.; Paik, C.Y.; Plys, M.G.; MAAP4-Modular Accident Analysis Program for LWR Plants, Fauske and Associates Inc., U.S.A, 1994.
8. Travis, J.R.; Royal, P.; Xiao, J.; Necker, G.A.; Reflinger, R.; Spore, J.W.; Lam, K.L.; Wilson, T.L.; Muller, C.; Nichols, B.D. GASFLOW: a Computational Fluid Dynamics Code for Gases, Aerosols, and Combustion, KIT, Germany, 2011

9. Yanez, J.; Kotchourko, A.; Lelyakin, J.; Hydrogen Deflagration Simulations under Typical Containment Conditions for Nuclear Safety. *Nuclear Eng. and Design* **2012**, 250, pp. 678-686.
10. Movahed-Shariat-Panahi, M.A.; Recommendation for Maximum Allowable Mesh Size for Plant Combustion Analyses with CFD codes. *Nuclear Eng. and Design* **2012**, 253, pp. 360-366.
11. Kotchourko, A.; Lelyakin, J. (KIT, Karlsruhe, Land Baden-Württemberg, Germany). Personal communication, 2016
12. Bentaib, A.; Bleyer, A.; Chaumeix, N.; Schramm, B.; Höhne, M.; Kostka, P.; Movahed, M.; Brähler, T.; Kang, H.S.; Kim, S.B.; Povilaitis, M.; Final Results of the SARNET Hydrogen Deflagration Benchmark Effect of Turbulence of Flame Acceleration. Proceedings of 5<sup>th</sup> ERMSAR-2012, Cologne, Germany, March 21-23, 2012.
13. Kotchourko, A.; Bentaib, A.; Fischer, K.; Chaumeix, N.; Yanez, J.; Benz, S.; Kudryakov, S.; ISP-49 on Hydrogen Combustion, Technical Report, NEA/CSNI/R(2011), OECD/NEA, 2012.
14. Kanzleiter, T.; Gupta, S.; Fisher, K.; Ahrens, G.; Langer, G.; Kuhnel, A.; Poss, G.; Hydrogen and Fission Product Issues Relevant for Containment Safety Assessment under Severe Accident Conditions, Final Report, 1501326-FR 1, OECD-NEA THAI Project, 2010.
15. Kang, H.S.; Hong, S.W.; CFD Analysis of Hydrogen Combustion under Spray Operation with a Modified TFC Model. Presentation at OECD/NEA THAI2 Project 6<sup>th</sup> Meeting, Eschborn, Germany, June 10-12, 2014.
16. Bentaib, A.; Cataldo, C.; Chaumont B.; Chevalier-Jabet, K.; Evaluation of the Impact PARs Have on the Hydrogen Risk in the Reactor Containment: Methodology and Application to PSA Level 2. *Science and Technology of Nuclear Installations* **2010**, 2010, pp. 1-7.
17. Kang, H.S.; Kim, J.; Kim, S.B, Hong, S.W.; Numerical Analysis for a Hydrogen Combustion Phenomenon in the APR1400 Containment during Severe Accidents Using a Multi-Dimensional Hydrogen Analysis System. Proceedings of the WORTH-8, Yeosu, Korea, Oct. 22-24, 2017.